Parameter Interpolation Adversarial Training for Robust Image Classification

Xin Liu, Yichen Yang, Kun He, *Senior Member, IEEE*, John E. Hopcroft, *Life Fellow, IEEE*

Abstract—Though deep neural networks exhibit superior performance on various tasks, they are still plagued by adversarial examples. Adversarial training has been demonstrated to be the most effective method to defend against adversarial attacks. However, existing adversarial training methods show that the model robustness has apparent oscillations and overfitting issues in the training process, degrading the defense efficacy. To address these issues, we propose a novel framework called Parameter Interpolation Adversarial Training (PIAT). PIAT tunes the model parameters between each epoch by interpolating the parameters of the previous and current epochs. It makes the decision boundary of model change more moderate and alleviates the overfitting issue, helping the model converge better and achieving higher model robustness. In addition, we suggest using the Normalized Mean Square Error (NMSE) to further improve the robustness by aligning the relative magnitude of logits between clean and adversarial examples rather than the absolute magnitude. Extensive experiments conducted on several benchmark datasets demonstrate that our framework could prominently improve the robustness of both Convolutional Neural Networks (CNNs) and Vision Transformers (ViTs).

Index Terms—Adversarial examples, adversarial training, parameter interpolation, normalized mean square error

I. INTRODUCTION

Deep Neural Networks (DNNs) have been widely used in various tasks, including computer vision [1]–[3], natural language processing [4], [5], and speech recognition [6], [7]. However, they are known to be vulnerable to adversarial examples by injecting malicious perturbations to clean examples that can cause the model to misclassify inputs with high confidence [8], [9]. Since DNNs have been applied in many safety systems, it is crucial to make them reliable and robust.

As the most effective defense approach, adversarial training dynamically generates adversarial examples and incorporates them during training. Recently, numerous adversarial training methods have been proposed to boost the model's performance, such as adding regularization term [10]–[15], assigning different weights to the data points [16], [17] and adapting to generate suitable adversarial examples [18]–[21]. However, the model robustness remains unsatisfactory due to hard convergence and generalization of adversarial training.
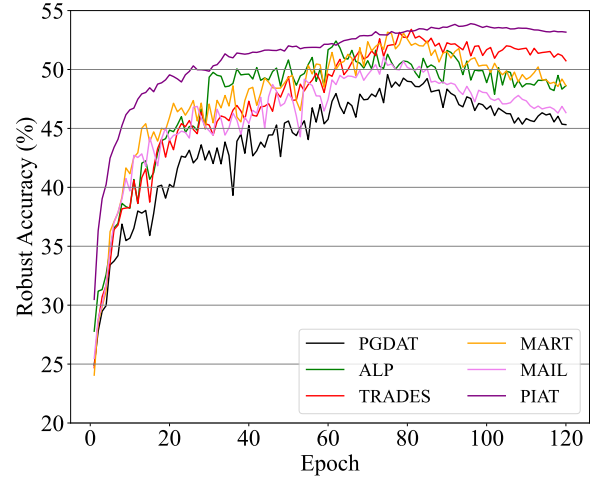
Fig. 1: The robust accuracy of ResNet18 trained on CIFAR10 dataset by existing advanced adversarial training methods has apparent oscillations and overfitting issues in the training process. On the contrary, our PIAT framework achieves excellent robust accuracy with better convergence, further improving the model performance.

Previous works [11], [22] have shown that adversarial training yields a more complex decision boundary than standard training. Moreover, we observe that the robust accuracy of the model has apparent oscillations in the early training stage, as illustrated in Fig. 1 Worse still, in the later training stage, the experiments show that the overfitting issue occurs. The training accuracy continues to increase, but the robust accuracy of the testing data begins to decline. Consequently, a natural intuition is that the model robustness can be improved if the adversarial training converges stably without overfitting.

Based on this motivation, we introduce a novel framework called Parameter Interpolation Adversarial Training (PIAT) to solve the apparent oscillations and overfitting issues of model robustness in the training process. Specifically, PIAT tunes the model parameters between each epoch by interpolating the model parameters of the previous and current epochs. To balance the effect of previous accumulated and current parameters, PIAT gradually increases the weight of the previous model parameters when tuning the current model parameters since the model parameters become more valuable during the course of training. In other words, PIAT focuses more on current model parameters in the early training stage to make

the model converge more stably. In the later training stage, PIAT focuses more on previously accumulated parameters, preventing the decision boundary from becoming too complex and alleviating the overfitting issue.

Moreover, there have been many works [10], [11], [23] proposed to encourage similarity between the output of clean and adversarial examples. Particularly, we observe that ALP [10] uses the mean square error loss to align the absolute magnitude of logits between clean and adversarial examples. However, the data distribution of clean and adversarial examples is quite different, and simply forcing the output to be close is too demanding. Therefore, we propose a new metric called Normalized Mean Square Error (NMSE) to align the clean and adversarial examples better. It pays more attention to aligning the relative magnitude rather than the absolute magnitude of logits.

Our main contributions are summarized as follows:

- To mitigate the oscillations and the overfitting issues in the training process, we propose the PIAT framework that interpolates the model parameters of the previous and current epochs. PIAT tunes the model parameters to converge stably, alleviates overfitting issues, and achieves higher robustness.
- We suggest using NMSE as a new regularization term to better align the clean and adversarial examples. NMSE pays more attention to the relative magnitude of the output of clean and adversarial examples rather than the absolute magnitude.
- Extensive experiments demonstrate that our method is an effective and general framework, achieving excellent robustness on both Convolutional Neural Networks (CNNs) and Vision Transformers (ViTs).

II. RELATED WORK

A. Adversarial Example

Let x_i and y_i denote a clean example and the corresponding ground-truth label in dataset $\mathcal{D} = (x_i, y_i)_{i=1}^{n}$, where $x_i \in \mathcal{X}$ and $y_i \in \mathcal{Y} = \{1, ..., c\}$. The goal of adversaries is to find an adversarial example $x_i^{adv} \in \mathcal{B}_\epsilon[x_i] = \{x_i^{adv} \| \|x_i^{adv} - x_i\|_\infty \leq \epsilon\}$, which causes errors in the model prediction.

Existing adversarial attacks can be categorized into white-box [8] and black-box attacks [24]. In general, the adversarial attacks can achieve good performance in the white-box setting, where the attacker can access the complete information of the target model, including the architecture and model weights.

Numerous methods have been proposed to improve the performance of adversarial examples in the white-box setting. The Fast Gradient Sign Method (FGSM) [8] is the first white-box attack that crafts adversarial examples by utilizing the sign of the gradient direction, formulated by:

$$x^{adv} = x + \epsilon \cdot \text{sign}(\nabla_x \mathcal{L}(f_\theta(x), y)), \qquad (1)$$

where x denotes the adversarial example, $\text{sign}(\cdot)$ is the signal function, and ϵ is the perturbation magnitude. Iterative Fast Gradient Sign Method (I-FGSM) [25] extends to an iteration version, which generates adversarial examples with multiple iterations and a smaller step size. Momentum Iterative Fast

Gradient Sign Method (MI-FGSM) [24] introduces momentum to enhance the transferability of adversarial examples as follows:

$$
\begin{aligned}
g_t &= \mu \cdot g_{t-1} + \frac{\nabla_x(\mathcal{L}(f_\theta(x_{t-1}^{adv}), y))}{\|\nabla_x(\mathcal{L}(f_\theta(x_{t-1}^{adv}), y))\|_1}, \\
x_t^{adv} &= x_{t-1}^{adv} + \alpha \cdot \text{sign}(g_t).
\end{aligned}
\qquad (2)
$$

where x_i^t denotes the adversarial example at the tth step, g_t is the gradient at the tth step, $\|\cdot\|_1$ is the 1-norm and α is the step size. Projected Gradient Descent (PGD) [26] generates stronger adversarial perturbation by means of multi-step iterative projection, formulated by:

$$x_i^{t+1} = \prod_{\mathcal{B}_\epsilon[x_i]} (x_i^t + \alpha \cdot \text{sign}(\nabla_{x_i^t} \mathcal{L}(f_\theta(x_i^t), y_i)), \qquad (3)$$

where x_i^t denotes the adversarial example at the tth step and $\prod(\cdot)$ is the projection operator, which constrains the magnitude of the perturbation range. The C&W attack [27], which generates adversarial examples by the optimization-based method, is widely used to evaluate the model robustness. AutoAttack (AA) [28] is a parameter-free ensemble attack, which has been widely adopted as one of the criteria for evaluating the model robustness.

B. Adversarial Training

Adversarial training (AT) has been demonstrated to be the most effective method to defend against adversarial examples. It dynamically generates adversarial examples and incorporates them during training to improve the robustness of DNNs. To achieve this goal, PGD-AT [26] formulates the adversarial training optimization problem as the following min-max problem:

$$\min_\theta \sum_i \max_{x_i^{adv} \in \mathcal{B}_\epsilon[x_i]} \mathcal{L}(f_\theta(x_i^{adv}), y_i), \qquad (4)$$

where $f_\theta(\cdot) : \mathbb{R}^d \to \mathbb{R}^c$ is the DNN classifier with parameter θ. $\mathcal{L}(\cdot, \cdot)$ represents the cross entropy loss.

PGD-AT introduces a new optimization paradigm, and along this multi-step paradigm, numerous works have been explored to further alleviate the adversarial vulnerability of DNNs. Adding regularization terms, such as ALP [10] and TRADES [11], provides a systematic way to better align the logits between clean and corresponding adversarial examples. MART [23] and MMA [29] explicitly differentiate the misclassified and correctly classified examples during training. RAT [30] further adds random noise to deterministic weights and using Taylor expansion, aiming to improve robustness against adversarial examples. To better utilize the model capacity, weighted adversarial training methods, such as GAIRAT [31] and MAIL [16], introduce a weighting strategy where the larger weight is assigned to more vulnerable pointers closer to the decision boundary. To achieve a better trade-off between robustness and accuracy, some methods, including LBGAT [32] and HAT [33], use the clean example output of the normally trained model to modify the adversarial example output of the adversarial trained model. MLCAT [34], UIAT [35], and STAT [36] focus on maximizing the likelihood

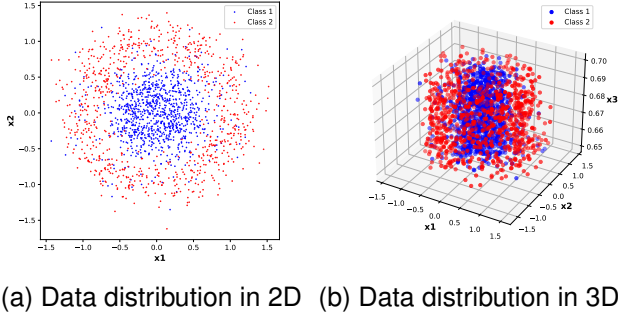(a) Data distribution in 2D (b) Data distribution in 3D

Fig. 2: The data distributions of the toy example, which is two concentric circles with different radii. The class 1 data are primarily located within the inner, while the class 2 data are mainly distributed on the outside.

of both adversarial examples and neighbouring data points. ARD and PRM [37] is the first work, which proposes using randomly masking gradients from some attention blocks or masking perturbations to improve the adversarial robustness of ViTs. CFA [38] customizes training configurations for different classes to enhance both robustness and fairness in adversarial training, addressing disparities in robustness among classes.

The works most related to ours are KDSWA [39] and ALP [10]. KDSWA [39] introduces SWA [40], which uses random weight average to smooth model weights and mitigates the overfitting issue. Instead of training one model and random ensemble on another like SWA, our PIAT framework interpolates the previous and current model parameters of the same model to achieve a more moderate change in the decision boundary at each epoch and continues to train the model using the interpolated parameters. Besides, ALP [10] calculates the regularization term using the absolute magnitude of logits with the MSE loss, while our NMSE focuses on aligning the relative magnitude.

III. MOTIVATION

In this section, we first construct a synthetic dataset and explore its decision boundary to investigate the solution for the apparent oscillation issue in adversarial training. Then, we provide some theoretical analysis in solving the overfitting issue in adversarial training. Finally, we rethink the alignment mode of ALP and present a novel regularization to align the logits between clean and adversarial examples.

A. A Toy Example

To delve into the techniques of adversarial training, we construct a simple 3D binary classification dataset comprising two distinct data distributions, specifically two concentric circles with different radii, and observe the accuracy and robustness of the model during the training process. Figure 2 illustrates the toy dataset in two dimensions (2D) and three dimensions (3D), respectively. The data used in the toy example comes from two different data distributions, shown by red points and blue points respectively. Specfically, we generate the
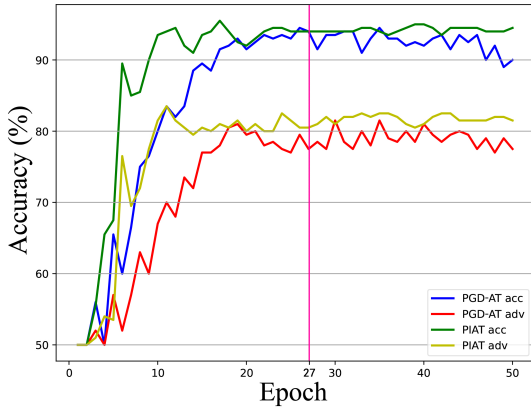
three features x_1, x_2 and x_3 using the following equations: $x_1 = \rho_i cos(z) + \epsilon_1, x_2 = \rho_i sin(z) + \epsilon_2, x_3 \sim U(\alpha_i, \beta_i)$, where $z \sim U(0, 2\pi)$ and $\epsilon_1, \epsilon_2 \sim N(0, \sigma_2)$. Here, $i = 1$ for class 1 and $i = 2$ for class 2. We set the parameters as follows: $\sigma = 0.2, \rho_1 = 0.35, \rho_2 = 1, \alpha_1 = \alpha_2 = 0.80$ and $\beta_1 = \beta_2 = 0.85$. We use a single hidden layer of MLP as the training model. For the model training, we use SGD with a momentum of 0.9 and a learning rate to 0.5. The learning rate value is chosen to reflect the convergence difficulty observed when training on other datasets such as CIFAR10 and CIFAR100. We train the model through adversarial training for 50 epochs and generate adversarial examples using a PGD attack. The attack parameters are set as follows: a step size of $\alpha = 0.05$, a maximum perturbation boundary of $\epsilon = 0.1$, and iterations $K = 5$ for the adversarial training.

As illustrated in Fig. 3, the robustness of the model trained by PGD-AT exhibits apparent oscillation during training. To further explore the reason for the oscillation issue, we observe the decision boundary of all the epochs where the robustness exhibits a sudden decrease. As shown in Fig. 4, taking the 27th epoch as an example, we observe that the decision boundary of model changes rapidly from the beginning to the end, leading to a significant fluctuation in the model robustness. However, we could not directly reduce the learning rate of the optimizer because this will slow down the convergence and cause the overfitting issue in the later stage.
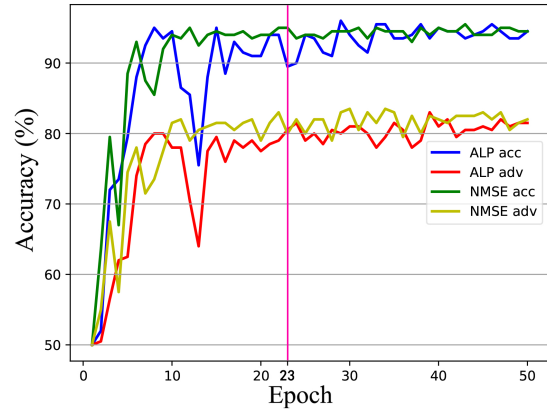
The aforementioned phenomenon raises an intriguing question: Can the model achieve improved adversarial robustness by converging more stably when the changes in the decision boundary are relatively smooth? To implement this idea of mitigating the dramatic change on decision boundary, we tune the model parameters at the end of each epoch by interpolating the model parameters of the previous and current epochs, leading to better initial model parameters for the next epoch.

We investigate the difference of decision boundary change between PGD-AT and our PIAT framework when the model robustness exhibits a sudden decline. To facilitate a more comprehensive comparison of the decision boundaries between PGD-AT and PIAT, we enhance the clarity by overlaying the decision boundary images before and after adversarial training. As illustrated in Fig. 5, we observe that the decision boundary change of PIAT framework is more moderate than that of PGD-AT when the model robustness exhibits a sudden decrease. Taking the 27th epoch as an example, although the blue data point located in the bottom left near the decision boundary can be classified correctly, some red data points situated in the top right and top left of the decision boundary are misclassified. On the other hand, taking the 25th epoch as an example, the decision boundary change in the model trained using the PIAT framework is moderate. As shown in Fig. 3, since the decision boundary change is more moderate, our method effectively enhances the model robustness while maintaining the accuracy of clean examples.

Moreover, we also observe the same phenomenon in the training process on CIFAR10 dataset. As shown in Fig. 1, typical advanced adversarial training methods also suffer from apparent oscillations and perform unsatisfactorily on the model robustness. Compared with these approaches, our method not

(a) The model trained by PGD-AT and PIAT

(b) The model trained by ALP and NMSE

Fig. 3: Illustrations of defense performance under PGD adversarial attack.The first figure illustrates the accuracy and robustness of the toy model trained using PGD-AT and PIAT on the 3D dataset, while the second figure demonstrates the accuracy and robustness of the toy model with ALP and NMSE regularization on the same dataset.
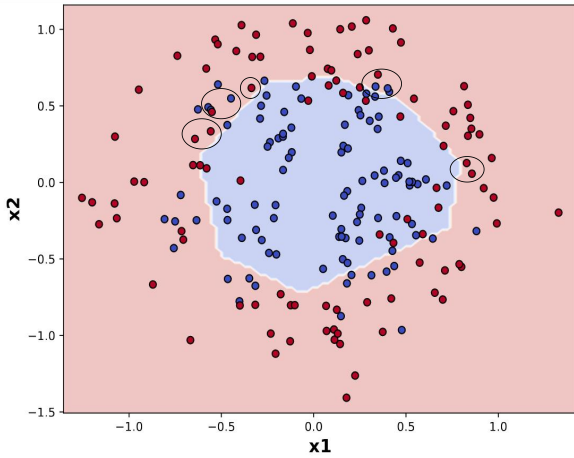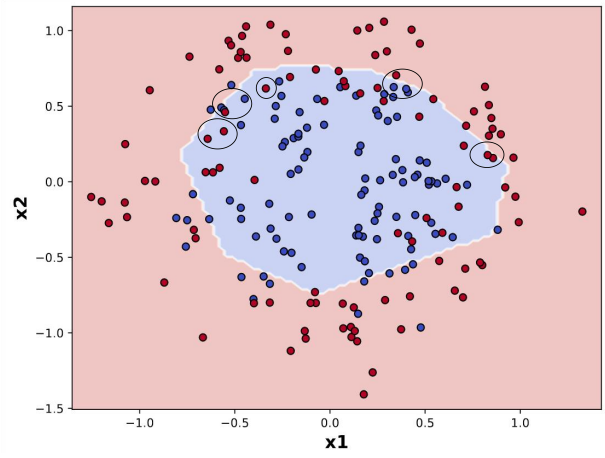

(a) The decision boundary before the 27th epoch

(b) The decision boundary after the 27th epoch

Fig. 4: Illustrations of the 2D decision boundary of the model trained using PGD-AT at the 27th epoch. The corresponding data points are marked by circles. While the blue data points near the top left of the decision boundary are correctly classified, the red data points situated around the top left and right are misclassified.

only alleviates the difficulty of convergence but also improves the performance of model.

Additionally, as illustrated in Fig. 1, our parameter interpolation method can also alleviate the overfitting issue in the later stage of the training. Theorem III-A provides the theoretical analysis of this phenomenon.

Theorem 3.1 *Assuming that for $i, j \in \{1, ..., T\}$, $\boldsymbol{\theta}_i = \boldsymbol{\theta}_j$ if and only if $i = j$. Model $f_{\boldsymbol{\theta}}$ is continuous and at least first-order differentiable. $f_{\tilde{\boldsymbol{\theta}}}$ is based on parameter interpolation $\tilde{\boldsymbol{\theta}} = \lambda \boldsymbol{\theta}_i + (1 - \lambda)\boldsymbol{\theta}_{i+1}$. The difference between the prediction of model $f_{\tilde{\boldsymbol{\theta}}}$ and model $f_{\boldsymbol{\theta}_i}$ is a first-order infinitesimal of λ if and only if $\lambda \to 1$.*

Proof. For the sake of the first differentiability of $f_{\boldsymbol{\theta}_{i+1}}(x, y)$, based on the Taylor expansion, we can fit a first

order polynomial of $f_{\boldsymbol{\theta}_{i+1}}(x, y)$ to approximate the value of $f_{\boldsymbol{\theta}_i}(x, y)$:

$$f_{\boldsymbol{\theta}_{i+1}}(x, y) = f_{\boldsymbol{\theta}_i}(x, y) + \Delta\boldsymbol{\theta}_1^T \nabla_{\boldsymbol{\theta}_i} f_{\boldsymbol{\theta}_i}(x, y) + O(\Delta\boldsymbol{\theta}_1^n), \quad (5)$$

where $\Delta\boldsymbol{\theta}_1 = \boldsymbol{\theta}_{i+1} - \boldsymbol{\theta}_i$ and $O(\Delta\boldsymbol{\theta}_1^n)$ represents the higher order remainder term. Note that the subscript $\Delta\boldsymbol{\theta}_1$ here stands for a neighborhood where the Taylor expansion approximates a function by polynomials of any point in terms of its value and derivatives. In the same way, we can get the first order polynomial of $f_{\tilde{\boldsymbol{\theta}}}(x, y)$ to approximate the value of $f_{\boldsymbol{\theta}_i}(x, y)$:

$$f_{\tilde{\boldsymbol{\theta}}}(x, y) = f_{\boldsymbol{\theta}_i}(x, y) + \Delta\boldsymbol{\theta}_2^T \nabla_{\boldsymbol{\theta}_i} f_{\boldsymbol{\theta}_i}(x, y) + O(\Delta\boldsymbol{\theta}_1^n), \quad (6)$$

where $\Delta\boldsymbol{\theta}_2 = \tilde{\boldsymbol{\theta}} - \boldsymbol{\theta}_i = (1 - \lambda)\Delta\boldsymbol{\theta}_1$. Therefore, the difference between the prediction of model $f_{\tilde{\boldsymbol{\theta}}}$ and model $f_{\boldsymbol{\theta}_i}$ can be

(a) PGD-AT from 26th to 27th epoch

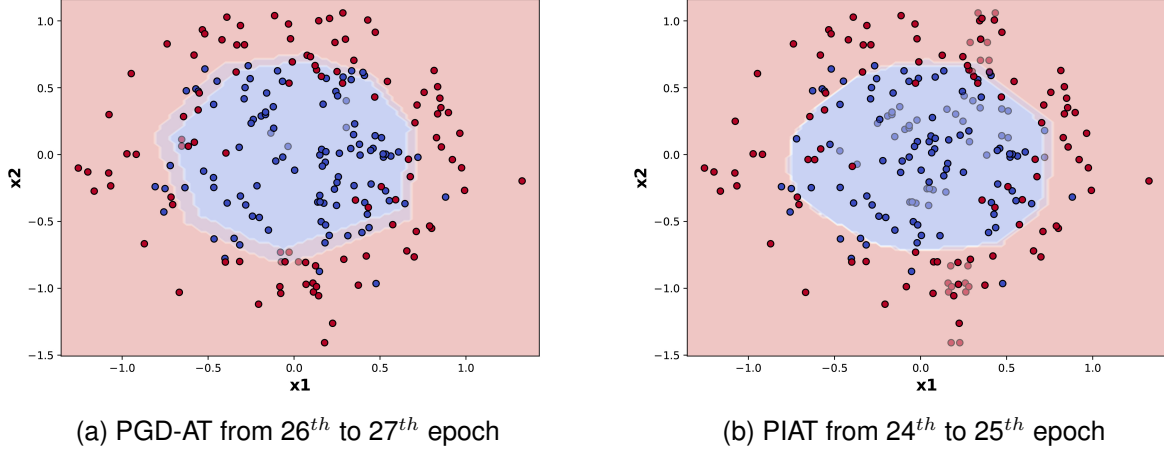(b) PIAT from 24th to 25th epoch

Fig. 5: Illustrations on the decision boundaries of PGD-AT and PIAT before/after an epoch. Each subfigure contains the decision boundary illustration before (in light-colored) and after (in dark-colored) the adversarial training. Specifically, the light-colored data represent the 26th epoch of PGD-AT and the 24th epoch of PIAT, while the dark-colored data correspond to the 27th epoch of PGD-AT and the 25th epoch of PIAT.

formulated as:

$$
\begin{aligned}
f_{\tilde{\boldsymbol{\theta}}}(x,y) - f_{\boldsymbol{\theta}_i}(x,y) &= \Delta\boldsymbol{\theta}_2^T \nabla_{\boldsymbol{\theta}_i} f_{\boldsymbol{\theta}_i}(x,y) + O(\Delta\boldsymbol{\theta}_2^n) \\
&= (1-\lambda)\Delta\boldsymbol{\theta}_1^T \nabla_{\boldsymbol{\theta}_i} f_{\boldsymbol{\theta}_i}(x,y) + O(\Delta\boldsymbol{\theta}_2^n) \\
&\leq \Delta\boldsymbol{\theta}_1^T \nabla_{\boldsymbol{\theta}_i} f_{\boldsymbol{\theta}_i}(x,y) + O(\Delta\boldsymbol{\theta}_1^n) \\
&= f_{\boldsymbol{\theta}_{i+1}}(x,y) - f_{\boldsymbol{\theta}_i}(x,y).
\end{aligned}
\tag{7}
$$

In the later stage, the model trained by standard adversarial training is overfitting. Meanwhile, the hyperparameter λ is close to 1. Thus, the prediction of model $f_{\tilde{\boldsymbol{\theta}}}$ is more similar to $f_{\boldsymbol{\theta}_i}$ instead of $f_{\boldsymbol{\theta}_{i+1}}$, alleviating the overfitting issue.

Theorem 3.1 indicates that the difference between the prediction of models $f_{\tilde{\boldsymbol{\theta}}}$ and $f_{\boldsymbol{\theta}_i}$ is smaller than that of $f_{\boldsymbol{\theta}_{i+1}}$ and $f_{\boldsymbol{\theta}_i}$ when λ is close to 1. This reveals the potential reason why the model trained by the parameter interpolation method does not cause the overfitting issue in the later stage.

B. Regularization of Aligning Logits

Here, we also conduct a similar experiment to study the robust improvement of the regularization. As shown in Fig. 3, although ALP can effectively boost model robustness, the model accuracy decreases apparently at the same time. Taking the 23th epoch as an example, the increase of model robustness comes at the sacrifice of accuracy. We revisit the robustness regularization of ALP, which can be formulated as follows:

$$
\mathcal{L}_{ALP} = \|f_{\boldsymbol{\theta}}(\boldsymbol{x}) - f_{\boldsymbol{\theta}}(\boldsymbol{x}^{adv})\|_2^2,
\tag{8}
$$

where $f_{\boldsymbol{\theta}}(\boldsymbol{x})$ is the output logits of the model, and $\|\cdot\|_2$ denotes l_2-norm. It might be attributed to the fact that clean and adversarial examples belong to different data distributions. Therefore, simply forcing the output logit to be close is unreasonable, which naturally leads to an opposed relationship between accuracy and robustness.

To maintain the model accuracy while boosting the robustness, we further customize a novel regularization term, which pays more attention to the relative magnitude of logits rather than absolute magnitude. As shown in Fig. 3, the model trained with our proposed regularization term improves model robustness while keeping the clean accuracy.

IV. METHODOLOGY

In this section, we introduce the realization of our Parameter Interpolation Adversarial Training (PIAT) framework and describe how to combine our proposed Normalized Mean Square Error (NMSE) regularization term to the framework.

A. The Proposed New Framework: PIAT

To mitigate the impact of the rapid changes in the model decision boundary, we propose a new framework called Parameter Interpolation Adversarial Training (PIAT). PIAT tunes the model parameters by interpolating the model parameters between the previous and current epochs. Mathematically, it can be formalized as follows:

$$
\boldsymbol{\theta}'_t = \lambda \cdot \boldsymbol{\theta}'_{t-1} + (1-\lambda) \cdot \boldsymbol{\theta}_t, \quad 0 \leq \lambda \leq 1,
\tag{9}
$$

where $\boldsymbol{\theta}'_{t-1}$ is the model parameters of the previous epoch after interpolation, and $\boldsymbol{\theta}_t$ is the current parameters at the end of the training epoch before interpolation. Before starting the next training epoch, we tune the model parameters to $\boldsymbol{\theta}'_t$. The hyper-parameter λ controls the tradeoff between previous and current parameters.

Based on the observations presented in Section III-A, we can gain an intuitive understanding the value of λ from two perspectives. Initially, when the model lacks robustness and informative parameters due to insufficient fitting to the training data. Therefore, λ should be set to a small value in the early stage. However, as the training progresses and the model

---

Algorithm 1 The PIAT Framework

Input: Initial model parameters $\boldsymbol{\theta}_0$, perturbation step size ϵ, number of adversarial attack steps K, number of epochs N, weight function $g(\cdot)$

Output: $\boldsymbol{\theta}'_N$

Initialize $\boldsymbol{\theta}'_0 \leftarrow \boldsymbol{\theta}_0$

for $i = 1$ **to** N **do**

    $\boldsymbol{\theta}_i \leftarrow \boldsymbol{\theta}'_{i-1}$

    for $minibatch \ \boldsymbol{x} \subset \boldsymbol{x}$ **do**

        $\boldsymbol{x}^{adv} \leftarrow \boldsymbol{x}$

        for $k = 1$ **to** K **do**

            $\boldsymbol{x}^{adv} \leftarrow \boldsymbol{x}^{adv} + \epsilon \cdot sign(\nabla_{\boldsymbol{x}} \mathcal{L}_{CE}(\boldsymbol{x}^{adv}, y))$

            $\boldsymbol{x}^{adv} \leftarrow clip(\boldsymbol{x}^{adv}, \boldsymbol{x} - \epsilon, \boldsymbol{x} + \epsilon)$

        end for

        $loss = \mathcal{L}(\boldsymbol{x}^{adv}, y)$

        update $\boldsymbol{\theta}_i$

    end for

    $\lambda \leftarrow g(i)$

    $\boldsymbol{\theta}'_i \leftarrow \lambda \cdot \boldsymbol{\theta}'_{i-1} + (1 - \lambda) \cdot \boldsymbol{\theta}_i$

end for

return $\boldsymbol{\theta}'_N$

---

becomes more adversarially robust, λ should be gradually increased towards 1 in the later stages of training.

According to the above analysis, λ should change over the course of training instead of using a fixed value. The value of λ should be small in the early training stage and gradually increase along with the training, ensuring the convergence speed and alleviating the overfitting issue in the adversarial training process. In this paper, we set λ as follows:

$$\lambda = g(n) = \frac{an + b}{cn + d}, \quad c \geq a, \quad d \geq b, \tag{10}$$

where n denotes the current number of training epochs. a, b, c and d are hyper-parameters and we set $a = b = c = 1$, $d = 10$ in this work.

Algorithm 1 summarizes the flexible framework of PIAT, which can seamlessly integrate with different adversarial training methods on both CNNs and ViTs without imposing restrictions on the choice of loss function or model.

B. The Proposed Regularization Term: NMSE

According to the discussion in Section III-B, instead of aligning the clean and adversarial examples by classification probabilities, we utilize the output logits normalized with l_2-norm.

We align the clean and adversarial examples by minimizing the mean square error between their normalized output logits. Besides, we set $(1 - p_{clean})$ as the weight for different adversarial examples so that the model will pay more attention to the clean examples that are vulnerable. We formulate the Normalized Mean Square Error (NMSE) regularization as follows:

$$\mathcal{L}_{NMSE} = (1 - p_{clean}) \cdot \left\| \frac{f_{\boldsymbol{\theta}}(\boldsymbol{x})}{||f_{\boldsymbol{\theta}}(\boldsymbol{x})||_2} - \frac{f_{\boldsymbol{\theta}}(\boldsymbol{x}^{adv})}{||f_{\boldsymbol{\theta}}(\boldsymbol{x}^{adv})||_2} \right\|_2^2, \tag{11}$$

where $\boldsymbol{x}^{adv}$ is the adversarial example, $f_{\boldsymbol{\theta}}(\boldsymbol{x})$ is the output logits of the model, and $|| \cdot ||_2$ denotes l_2-norm.

In summary, the overall loss function in our PIAT framework with NMSE is as follows:

$$\mathcal{L} = \mathcal{L}_{CE} + \mu \cdot \mathcal{L}_{NMSE}, \tag{12}$$

where μ is a hyper-parameter to trade off the cross entropy loss $\mathcal{L}_{CE}$ on adversarial examples and the NMSE regularization term $\mathcal{L}_{NMSE}$. Moreover, we could replace the loss function in PIAT framework to combine with various AT methods.

V. EXPERIMENTS

A. Experimental Setup

Datasets and Models. Following the setting on Generalist [41], we conduct experiments on three benchmark datasets including CIFAR10, CIFAR100 [42], and SVHN [43] under L_∞ norm. The CIFAR10 contains 60000 color images with the size of 32×32 in 10 classes. The CIFAR100 shares the same setting as CIFAR10, except it owns 100 classes consisting of 600 images each. In CIFAR10 and CIFAR100 datasets, 50000 images are for training, and 10000 images are for testing the performance. SVHN is a dataset of street view house numbers, which includes 73257 examples for training and 26032 examples for evaluation. All images are normalized into $[0, 1]$. We do the evaluation on two CNNs and three ViTs, including ResNet18 [1], Wide-ResNet-32-10 (WRN-32-10) [44] and ViT [45], DeiT [46], ConViT [47], to verify the efficacy of our method.

Training and Evaluation Settings. For all the experiments of CNNs, we train ResNet18 (WRN-32-10) using SGD with a momentum of 0.9 for 120 (180) epochs. The weight decay is 3.5×10^{-3} for ResNet18 and 7×10^{-4} for WRN-32-10 on the three datasets. The initial learning rate for ResNet18 (WRN-32-10) is 0.01 (0.1) till epoch 60 (90) and then linearly decays to 0.001 (0.01), 0.0001 (0.001) at epoch 90 (135) and 120 (180). We adopt PGD attack with 10 steps for adversary generation during the training stage. The maximum adversarial perturbation of each pixel is $\epsilon = 8/255$ with the step size $\alpha = 2/255$. For the TRADES baseline, we adopt $\beta = 6$ for the best robustness. For the NMSE regularization term, we set $\mu = 5$ to achieve the best performance.

For the experiments of ViT (ConViT-Base, ViT-Base, DeiT-Small), we follow the previous setting [37] to finetune the various ViTs. Specifically, models are pre-trained on ImageNet-1K and are adversarially trained for 40 epochs using SGD with weight decay 1×10^{-4}, and an initial learning rate of 0.1 that is divided by 10 at the 36th and 38th epochs. Simple data augmentations such as random crop with padding and random horizontal flips are applied.

We compare the PIAT integrated with NMSE regularization with the following AT baselines: ALP [10], TRADES [11], MART [23], MAIL [16], CFA [38], RAT [30] on CNNs. Moreover, we also evaluate the performance of PIAT integrated with ARD and PRM (A&P) [37] on ViTs. We adopt various adversarial attacks to evaluate the defense efficacy of our method, including PGD [26], CW [27] and AutoAttack (AA) [28].

TABLE I: The clean and robust accuracy (%) of our methods (PIAT+NMSE) and defense baselines using ResNet18 model trained on CIFAR10, CIFAR100 and SVHN datasets under various adversarial attacks. We report the results of the best checkpoint according to the highest robust accuracy under PGD20 attack and the final checkpoint. The best result among defense methods in each column is in **bold**.

Dataset	Method	Clean			PGD20			CW			AA		
		Best	Final	Diff	Best	Final	Diff	Best	Final	Diff	Best	Final	Diff
CIFAR10	PGD-AT	**84.28**	**85.62**	1.34	50.29	45.86	4.43	49.31	43.25	6.06	46.33	41.36	4.97
	ALP	79.74	81.45	1.71	52.37	48.62	3.75	49.60	43.87	5.73	46.13	41.88	4.25
	TRADES	82.39	83.04	**0.65**	53.60	50.74	2.86	50.90	49.04	1.86	48.04	46.80	1.24
	MART	81.91	83.99	2.08	53.70	48.63	5.07	49.35	44.92	4.43	47.45	43.65	3.80
	MAIL	82.65	85.17	2.49	51.15	47.14	4.01	48.88	44.38	4.50	45.16	43.02	2.14
	CFA	82.80	83.88	1.08	53.24	51.69	1.55	51.45	49.97	1.48	48.40	47.74	**0.64**
	RAT	81.63	82.61	0.98	52.25	50.09	2.16	49.47	47.93	1.54	45.20	44.30	0.90
	PIAT +NMSE	80.96	82.84	1.88	**53.74**	**52.81**	**0.93**	**51.72**	**50.49**	**1.23**	**48.80**	**47.97**	0.83
CIFAR100	PGD-AT	58.48	58.53	**0.05**	28.36	21.72	6.64	27.06	21.12	5.94	23.85	19.55	4.30
	ALP	57.29	58.65	1.36	28.12	24.66	3.46	26.84	22.17	4.67	23.57	20.49	3.08
	TRADES	56.71	56.32	0.39	29.19	27.70	1.49	26.05	24.53	1.52	23.91	22.70	1.21
	MART	55.26	57.77	2.51	30.10	25.96	4.14	26.30	23.79	2.51	24.13	22.35	1.78
	MAIL	**58.73**	59.00	0.27	27.99	24.69	3.30	26.28	23.37	2.91	22.50	20.86	1.64
	CFA	56.28	**61.62**	5.34	30.64	29.74	0.90	27.74	25.95	1.79	24.26	21.58	2.68
	RAT	53.35	56.35	3.00	28.69	27.67	1.02	25.52	23.69	1.83	23.10	22.40	**0.70**
	PIAT +NMSE	56.04	57.16	1.12	**31.45**	**30.87**	**0.58**	**28.74**	**27.76**	**1.02**	**26.09**	**25.13**	0.96
SVHN	PGD-AT	**93.85**	**94.33**	0.48	59.01	52.35	6.66	48.66	44.13	4.53	43.02	38.66	4.36
	ALP	92.54	93.67	1.13	59.13	55.12	5.01	52.22	48.53	3.69	45.67	42.41	3.26
	TRADES	90.88	91.34	**0.46**	59.50	57.04	2.46	52.76	50.42	2.34	46.59	44.87	1.72
	MART	90.84	92.95	2.11	57.70	54.29	3.41	52.95	50.09	2.86	46.98	43.75	3.23
	MAIL	90.15	93.69	3.54	57.47	54.60	3.14	52.78	49.73	3.05	46.26	41.24	5.02
	CFA	92.23	93.68	1.45	60.77	58.85	1.92	55.17	52.71	2.46	49.64	46.53	3.11
	RAT	89.23	90.97	1.74	45.83	38.25	7.58	44.15	32.71	11.44	46.10	22.40	23.70
	PIAT +NMSE	91.70	93.07	1.37	**61.21**	**59.84**	**1.37**	**55.88**	**54.45**	**1.43**	**51.29**	**49.82**	**1.47**

B. Evaluation on Defense Efficacy

We compare the defense efficacy of our method with four AT baselines including PGD-AT, TRADES, MART, MAIL. Table I reports the best and final clean and robust accuracy of the ResNet18 model trained using our method or the defense baselines under various adversarial attacks on three datasets.

As shown in Table I, our method exhibits the best robustness on all three datasets under PGD20, CW and AA attacks . Specifically, our method achieves 48.80%, 26.09% and 51.29% accuracy under the AA attack, surpassing the best results of other defense baselines by 0.40%, 1.96%, 2.17%, respectively. Notably, the exceptional performance of our method on CIFAR100 highlights its generalizability in handling more complex datasets with a greater number of classes.

Moreover, our experimental results actually verify Theorem III-A, which reveals that our method can mitigate overfitting issues in adversarial training. As shown in Table I, our method achieves superior robust accuracy compared to the defense baselines on both the best and the final checkpoints with a minimal gap in robustness between them, indicating that the robustness of the model remains stable during training and the overfitting issue is alleviated.

To further investigate the effectiveness of our method with different network architectures, we conduct similar experiments using the WRN-32-10 model. As depicted in Table II,

the results indicate that our method still outperforms the competitors under the PGD and AA attacks, confirming its effectiveness even as the size of the DNN model scales up.

C. Ablation Study

PIAT Framework. Since PIAT is a general framework, we incorporate other adversarial training methods into PIAT to demonstrate its defense efficacy. Specifically, we evaluate the robust accuracy of the PIAT framework combined with PGD-AT, ALP, TRADES, MART, and MAIL under the AA attack on three datasets, respectively. As shown in Fig. 6, PIAT boosts the robustness of various adversarial training methods against the AA attack over all the three datasets with ResNet18 model. The results demonstrate that we can easily incorporate other adversarial training methods into our PIAT framework without incurring any additional cost to achieve better performance.

We also conduct similar experiments on the WRN-32-10 model and three different ViTs. We report the results in Table III and Table IV, respectively. Our PIAT framework integrated with other adversarial training methods significantly enhances the robust accuracy while maintaining the clean accuracy. For the WRN-32-10 model, when integrated with PIAT, the original adversarial training methods gain an improvement of 0.57%, 2.67%, 3.35%, 3.26% and 4.96%, respectively, under AA attack. Similarly, the combination of A&P

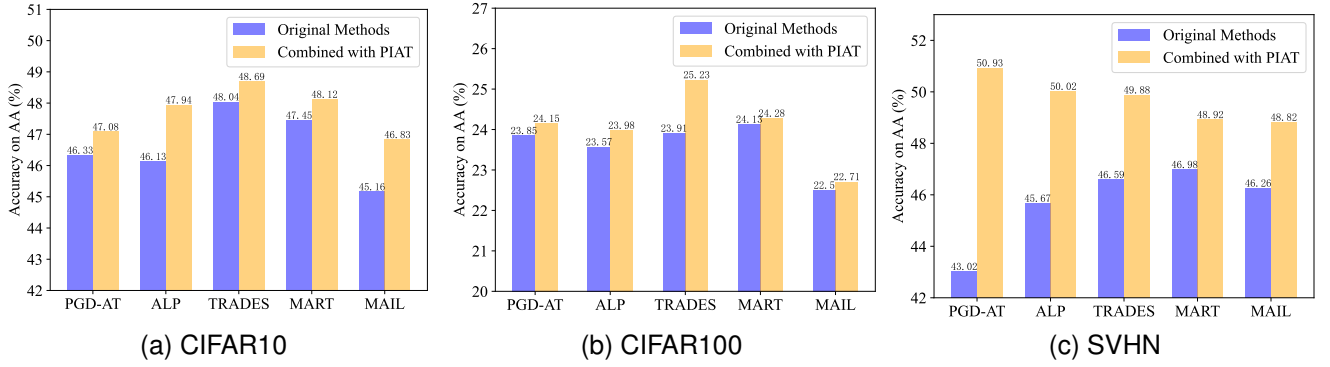(a) CIFAR10   (b) CIFAR100   (c) SVHN

Fig. 6: The robust accuracy (%) of the PIAT framework combined with various adversarial training baseline methods under the AA attack on CIFAR10, CIFAR100, and SVHN datasets using ResNet18 model.

TABLE II: The clean and robust accuracy (%) of our methods (PIAT+NMSE) and defense baselines using WRN-32-10 model on CIFAR10 and CIFAR100 datasets. The best result in each column is in **bold**.

Dataset	Method	Clean	PGD20	AA
CIFAR10	PGD-AT	**86.87**	48.77	47.78
	ALP	84.18	53.55	49.68
	TRADES	82.13	55.14	50.38
	MART	81.57	56.44	49.58
	MAIL	84.96	52.58	47.26
	CFA	86.44	57.84	52.96
	RAT	83.46	57.07	51.56
	PIAT +NMSE	85.04	**58.04**	**53.83**
CIFAR100	PGD-AT	59.30	28.13	23.99
	ALP	58.11	28.59	24.45
	TRADES	57.99	31.97	26.76
	MART	55.19	31.16	26.46
	MAIL	58.04	29.50	23.97
	CFA	**63.37**	33.89	28.98
	RAT	60.89	33.39	27.95
	PIAT +NMSE	61.04	**35.15**	**30.07**

TABLE III: The clean and robust accuracy (%) of PIAT framework combined with various adversarial training methods on CIFAR10 and CIFAR100 dataset using WRN-32-10 model. The best result among defense methods in each column is in **bold**.

Dataset	Method	Clean	PGD20	AA
CIFAR10	PGD-AT	**86.87**	48.77	47.78
	PIAT	85.56	**52.80**	**48.35**
	ALP	**84.18**	53.55	49.68
	PIAT+ALP	83.35	**57.71**	**52.35**
	TRADES	**82.13**	55.14	50.38
	PIAT+TRADES	82.08	**58.93**	**53.73**
	MART	**81.57**	56.44	49.58
	PIAT+MART	79.88	**59.51**	**52.84**
	MAIL	**84.96**	52.58	47.26
	PIAT+MAIL	84.24	**57.53**	**52.22**
CIFAR100	PGD-AT	59.30	28.13	23.99
	PIAT	**60.09**	**34.46**	**29.47**
	ALP	58.11	28.59	24.45
	PIAT+ALP	**59.25**	**34.04**	**28.94**
	TRADES	57.99	31.97	26.76
	PIAT+TRADES	**59.78**	**34.52**	**29.25**
	MART	**55.19**	31.16	26.46
	PIAT+MART	54.32	**34.87**	**28.79**
	MAIL	58.04	29.50	23.97
	PIAT+MAIL	**58.52**	**33.65**	**28.00**

and PIAT significantly enhances the robustness of ViTs, gaining an improvement of 2.85%, 2.24%, and 2.78%, respectively, against AA attacks for ConViT-B. Our framework leads to higher robust accuracy when combined with other adversarial training methods on both CNNs and ViTs, indicating that PIAT has good flexibility and generalization.

To evaluate the effectiveness of our PIAT framework on different datasets, we also compare the defense performance when combined PIAT with other baseline methods. As shown in Table III, our PIAT framework demonstrates a significantly enhancement in the robustness of the model. Specifically, when combined with the baseline methods, the original baseline methods gain an improvement of 5.48%, 4.49%, 2.49%, 2.33%, and 4.03% under AA attack, respectively. The results indicate that our PIAT framework is general and effective on different DNNs.

NMSE Regularization. To evaluate the effectiveness of our proposed NMSE regularization, we compare the performance of PGD-AT with ALP [10] and NMSE regularization, respectively. Table V presents the accuracy of the ResNet18 model against PGD and AA attacks. Specifically, the experimental results show that NMSE regularization achieves an absolute improvement of 0.47% and 1.25% under AA attack on CIFAR-10 and CIFAR-100, respectively. The experimental results demonstrate that our NMSE regularization surpasses ALP in

TABLE IV: The clean and robust accuracy (%) of PIAT framework combined with other adversarial training methods using ViTs on CIFAR10 dataset. Note that 'B' denotes 'base', 'S' denotes 'small'. The best result in each column is highlighted in **bold**.

Model	Method	Clean	PGD20	AA
ConViT-B	PGD-AT	61.47	38.64	34.07
	A&P	85.21	53.25	49.01
	PIAT+A&P	**87.50**	**56.25**	**51.86**
	TRADES	82.75	52.77	49.61
	A&P	83.51	53.21	50.11
	PIAT+A&P	**86.03**	**55.88**	**52.35**
	MART	63.61	42.51	37.08
	A&P	80.32	53.11	48.35
	PIAT+A&P	**81.20**	**56.17**	**51.13**
ViT-B	PGD-AT	83.07	52.93	48.99
	A&P	84.64	53.44	49.67
	PIAT+A&P	**87.83**	**56.34**	**52.27**
	TRADES	83.45	53.07	49.76
	A&P	83.91	53.52	50.56
	PIAT+A&P	**87.09**	**55.97**	**52.57**
	MART	77.05	52.99	47.95
	A&P	78.75	53.51	49.01
	PIAT+A&P	**82.23**	**55.94**	**51.03**
DeiT-S	PGD-AT	81.36	47.94	47.28
	A&P	83.08	52.28	47.92
	PIAT+A&P	**83.22**	**53.55**	**49.31**
	TRADES	82.32	52.52	49.07
	A&P	82.81	52.74	49.40
	PIAT+A&P	**83.43**	**53.31**	**50.10**
	MART	76.77	52.06	47.06
	A&P	**78.43**	52.98	47.94
	PIAT+A&P	78.39	**53.83**	**48.97**

TABLE V: The clean and robust accuracy (%) of NMSE and ALP under adversarial attacks on CIFAR10 and CIFAR100 datasets with ResNet18 model. The best result among defense methods in each column is in **bold**.

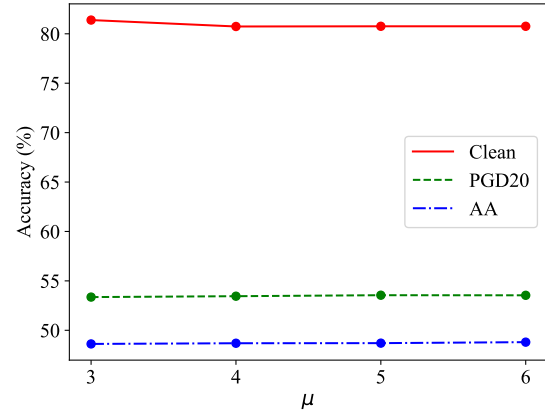| Dataset	Method	Clean	PGD20	AA
CIFAR10	ALP	79.74	**52.37**	46.13
	NMSE	**84.77**	51.56	**46.60**
CIFAR100	ALP	57.29	28.12	23.57
	NMSE	**58.88**	**29.55**	**24.82**

Fig. 7: The clean and robust accuracy (%) on CIFAR10 dataset for different hyper-parameters of the NMSE regularization term when combined with the PIAT framework. The performance of NMSE indicates the robustness of the hyper-parameter μ.

both clean accuracy and robust accuracy. Moreover, the improvements achieved by NMSE regularization are significant, highlighting its effectiveness in enhancing model robustness against strong adversarial attacks. The superior performance indicates the potential of NMSE regularization as a reliable method for improving the adversarial robustness of DNNs.

D. Further Study

Hyper-parameter of NMSE. The hyper-parameter μ in Eq. 12 trades off the cross-entropy loss and the NMSE regularization term for adversarial examples. To investigate the impact of different μ values on the accuracy of the PIAT framework combined with NMSE, we conduct a series of experiments on the CIFAR10 dataset. Fig. 7 presents the results on the CIFAR10 dataset when we take $\mu = 3, 4, 5, 6$. It demonstrates that the defense effectiveness of our method remains relatively stable across different μ values. This stability indicates that

our NMSE regularization term is robust to variations in the μ hyper-parameter. Given these observations, we choose $\mu = 5$ for our experiments, as this value provides an optimal balance between maintaining accuracy on clean examples and robustness against adversarial attacks. The robustness of our method to different μ values highlights the effectiveness and reliability of the NMSE regularization term with the PIAT framework.

Hyper-parameter of PIAT. The hyper-parameter λ in Eq. 9 controls the trade-off between model parameters from the previous and current epochs. In Section IV-A, we propose dynamically adjusting λ throughout the training instead of using a fixed value. To validate our assumption, we evaluate the clean and robust accuracy of PIAT combined with NMSE under PGD20 attack, comparing fixed λ values to our variable λ as defined in Eq. 10. As illustrated in Fig. 9, during the early stage of training, using a small fixed λ exhibits better model robustness and efficiency compared to a large fixed λ. However, in the later stage, the interpolation with a large fixed λ does not exhibit overfitting issues, which differs from the small fixed λ. These observations indicate that appropriately adjusting λ crucial. A dynamic λ alleviates oscillations in the early stage and address the overfitting issues in the later stages of the adversarial training process. Thus, the

(a) Loss landscape of PGD-AT
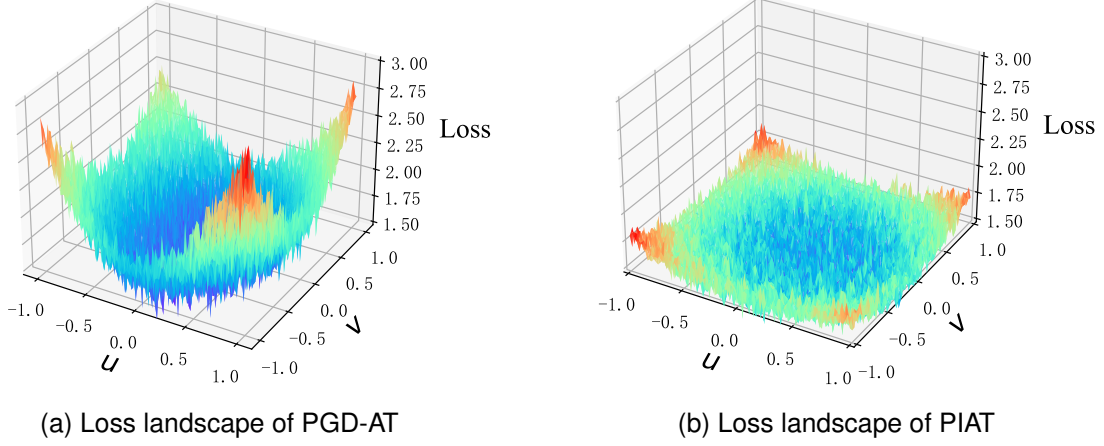

(b) Loss landscape of PIAT

Fig. 8: Illustrations of the loss landscape of PGD-AT and PIAT in 3D. The loss landscape of standard adversarially trained model changes dramatically, while our PIAT's changes smoothly, indicating that the model parameters trained by PIAT converge better to the flatter region.
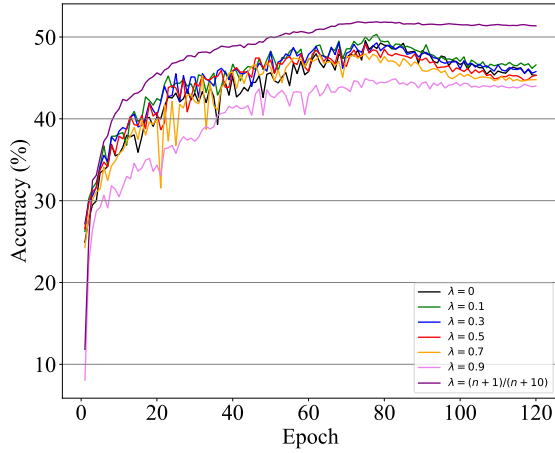

Fig. 9: The robust accuracy (%) on adversarial examples of ResNet18 model trained by PIAT with different λ on the CIFAR10 dataset. n denotes the current number of training epochs.

dynamic adjustment plays a key role in enhancing the overall effectiveness and robustness of the model.

E. Loss Landscape

To provide a comprehensive evaluation of the efficacy of our PIAT framework, we compare the loss landscape of models trained using the PIAT framework and PGD-AT in 3D. Let $\boldsymbol{u}$ and $\boldsymbol{v}$ be two random direction vectors sampled from the Gaussian distribution. We plot the loss landscape around $\boldsymbol{\theta}$ using the following equation while inputting the same data, where $m_1, m_2 \in [-1, 1]$:

$$\mathcal{L}(\boldsymbol{\theta}; \boldsymbol{u}; \boldsymbol{v}) = \mathcal{L}\left(\boldsymbol{\theta} + m_1 \frac{\boldsymbol{u}}{||\boldsymbol{u}||} + m_2 \frac{\boldsymbol{v}}{||\boldsymbol{v}||}\right). \quad (13)$$

As illustrated in Fig. 8, we observe that compared with PGD-AT, the model trained using the PIAT framework exhibits less fluctuation in the loss landscape with the changes in

model parameters under PGD20 attack . Furthermore, in comparison to the landscape obtained using PGD-AT, the landscape resulting from the PIAT framework suggests that the model converges to a flatter region. The flatter region signifies a higher level of robust accuracy, indicating that our PIAT framework improves model stability against adversarial perturbations. The stability implies that the PIAT framework not only improves robustness but also contributes to better generalization and resilience of the model. Additionally, the loss landscape of PGD-AT and PIAT framework have similar pattern in other adversarial attacks.

VI. CONCLUSION

To mitigate the oscillation and overfitting issues during the training process, we proposed a novel adversarial training framework called PIAT, which interpolates parameter interpolation between previous and current epochs. Furthermore, we suggested using Normalized Mean Squared Error (NMSE) as a regularization term to align the output of clean and adversarial examples. NMSE focuses on the relative magnitude of the logits rather than the absolute magnitude. Extensive experiments conducted on multiple benchmark datasets demonstrate the effectiveness of our framework in enhancing the robustness of both Convolutional Neural Networks (CNNs) and Vision Transformers (ViTs). Moreover, PIAT is flexible and versatile, allowing for the integration of various adversarial training methods into our framework to further boost the performance.

Compared to other methods, our approach can further enhance the adversarial robustness of the model without changing the existing adversarial training framework. We hope that future research will lead to more universal adversarial training frameworks that can further improve classification accuracy as well as robustness of the models.

REFERENCES

[1] K. He, X. Zhang, S. Ren, and J. Sun, "Deep residual learning for image recognition," in *Proceedings of the IEEE/CVF Conference on Computer Vision and Pattern Recognition*, 2016, pp. 770–778.

[2] A. Krizhevsky, I. Sutskever, and G. E. Hinton, "Imagenet classification with deep convolutional neural networks," in *Neural Information Processing Systems*, 2012, pp. 1106–1114.

[3] J. Long, E. Shelhamer, and T. Darrell, "Fully convolutional networks for semantic segmentation," in *Proceedings of the IEEE/CVF Conference on Computer Vision and Pattern Recognition*, 2015, pp. 3431–3440.

[4] J. Devlin, M. Chang, K. Lee, and K. Toutanova, "BERT: pre-training of deep bidirectional transformers for language understanding," in *Conference of the North American Chapter of the Association for Computational Linguistics: Human Language Technologies*, 2019, pp. 4171–4186.

[5] A. Vaswani, N. Shazeer, N. Parmar, J. Uszkoreit, L. Jones, A. N. Gomez, L. Kaiser, and I. Polosukhin, "Attention is all you need," in *Neural Information Processing Systems*, 2017, pp. 5998–6008.

[6] H. Sak, A. W. Senior, K. Rao, and F. Beaufays, "Fast and accurate recurrent neural network acoustic models for speech recognition," in *INTERSPEECH*, 2015, pp. 1468–1472.

[7] X. Chen, A. Ragni, X. Liu, and M. J. F. Gales, "Investigating bidirectional recurrent neural network language models for speech recognition," in *Conference of the International Speech Communication Association*, 2017, pp. 269–273.

[8] I. J. Goodfellow, J. Shlens, and C. Szegedy, "Explaining and harnessing adversarial examples," in *International Conference on Learning Representations*, 2015.

[9] K. Mahmood, R. Mahmood, and M. Van Dijk, "On the robustness of vision transformers to adversarial examples," in *IEEE/CVF International Conference on Computer Vision*, 2021, pp. 7838–7847.

[10] H. Kannan, A. Kurakin, and I. J. Goodfellow, "Adversarial logit pairing," *CoRR*, 2018.

[11] H. Zhang, Y. Yu, J. Jiao, E. P. Xing, L. E. Ghaoui, and M. I. Jordan, "Theoretically principled trade-off between robustness and accuracy," in *International Conference on Machine Learning*, 2019, pp. 7472–7482.

[12] T. Miyato, S.-I. Maeda, M. Koyama, and S. Ishii, "Virtual adversarial training: A regularization method for supervised and semi-supervised learning," *IEEE Transactions on Pattern Analysis and Machine Intelligence*, vol. 41, no. 8, pp. 1979–1993, 2019.

[13] Z. Yang, Q. Xu, W. Hou, S. Bao, Y. He, X. Cao, and Q. Huang, "Revisiting auc-oriented adversarial training with loss-agnostic perturbations," *IEEE Trans. Pattern Anal. Mach. Intell.*, vol. 45, no. 12, pp. 15 494–15 511, 2023.

[14] H. Ma, K. Xu, X. Jiang, Z. Zhao, and T. Sun, "Transferable black-box attack against face recognition with spatial mutable adversarial patch," *IEEE Trans. Inf. Forensics Secur.*, vol. 18, pp. 5636–5650, 2023.

[15] J. Liu, C. P. Lau, H. Souri, S. Feizi, and R. Chellappa, "Mutual adversarial training: Learning together is better than going alone," *IEEE Trans. Inf. Forensics Secur.*, vol. 17, pp. 2364–2377, 2022.

[16] F. Liu, B. Han, T. Liu, C. Gong, G. Niu, M. Zhou, M. Sugiyama *et al.*, "Probabilistic margins for instance reweighting in adversarial training," *Neural Information Processing Systems*, pp. 23 258–23 269, 2021.

[17] T. Lin, Y. Lee, F. Chang, J. M. Chang, and P. Wu, "Protecting sensitive attributes by adversarial training through class-overlapping techniques," *IEEE Trans. Inf. Forensics Secur.*, vol. 18, pp. 1283–1294, 2023.

[18] S. Lee, H. Lee, and S. Yoon, "Adversarial vertex mixup: Toward better adversarially robust generalization," in *Proceedings of the IEEE/CVF Conference on Computer Vision and Pattern Recognition*, 2020, pp. 269–278.

[19] J. Zhang, X. Xu, B. Han, G. Niu, L. Cui, M. Sugiyama, and M. S. Kankanhalli, "Attacks which do not kill training make adversarial learning stronger," in *International Conference on Machine Learning*, 2020, pp. 11 278–11 287.

[20] X. Jia, Y. Zhang, X. Wei, B. Wu, K. Ma, J. Wang, and X. Cao, "Improving fast adversarial training with prior-guided knowledge," *IEEE Transactions on Pattern Analysis and Machine Intelligence*, pp. 1–18, 2024.

[21] X. Yuan, Z. Zhang, X. Wang, and L. Wu, "Semantic-aware adversarial training for reliable deep hashing retrieval," *IEEE Trans. Inf. Forensics Secur.*, vol. 18, pp. 4681–4694, 2023.

[22] Y. Dong, K. Xu, X. Yang, T. Pang, Z. Deng, H. Su, and J. Zhu, "Exploring memorization in adversarial training," in *International Conference on Learning Representations*, 2022.

[23] Y. Wang, D. Zou, J. Yi, J. Bailey, X. Ma, and Q. Gu, "Improving adversarial robustness requires revisiting misclassified examples," in *International Conference on Learning Representations*, 2020.

[24] Y. Dong, F. Liao, T. Pang, H. Su, J. Zhu, X. Hu, and J. Li, "Boosting adversarial attacks with momentum," in *Proceedings of the IEEE/CVF Conference on Computer Vision and Pattern Recognition*, 2018, pp. 9185–9193.

[25] A. Kurakin, I. J. Goodfellow, and S. Bengio, "Adversarial examples in the physical world," in *International Conference on Learning Representations Workshop Track Proceedings*, 2017.

[26] A. Madry, A. Makelov, L. Schmidt, D. Tsipras, and A. Vladu, "Towards deep learning models resistant to adversarial attacks," in *International Conference on Learning Representations*, 2018.

[27] N. Carlini and D. A. Wagner, "Towards evaluating the robustness of neural networks," in *IEEE Symposium on Security and Privacy*, 2017, pp. 39–57.

[28] F. Croce and M. Hein, "Reliable evaluation of adversarial robustness with an ensemble of diverse parameter-free attacks," in *International Conference on Machine Learning*, 2020, pp. 2206–2216.

[29] G. W. Ding, Y. Sharma, K. Y. C. Lui, and R. Huang, "MMA training: Direct input space margin maximization through adversarial training," in *International Conference on Learning Representations*, 2020.

[30] G. Jin, X. Yi, D. Wu, R. Mu, and X. Huang, "Randomized adversarial training via taylor expansion," in *CVPR*, 2023, pp. 16 447–16 457.

[31] J. Zhang, J. Zhu, G. Niu, B. Han, M. Sugiyama, and M. S. Kankanhalli, "Geometry-aware instance-reweighted adversarial training," in *International Conference on Learning Representations*, 2021.

[32] J. Cui, S. Liu, L. Wang, and J. Jia, "Learnable boundary guided adversarial training," in *IEEE/CVF International Conference on Computer Vision*, 2021, pp. 15 701–15 710.

[33] R. Rade and S. Moosavi-Dezfooli, "Reducing excessive margin to achieve a better accuracy vs. robustness trade-off," in *International Conference on Learning Representations*, 2022.

[34] C. Yu, B. Han, L. Shen, J. Yu, C. Gong, M. Gong, and T. Liu, "Understanding robust overfitting of adversarial training and beyond," in *International Conference on Machine Learning*, K. Chaudhuri, S. Jegelka, L. Song, C. Szepesvári, G. Niu, and S. Sabato, Eds., 2022, pp. 25 595–25 610.

[35] J. Dong, S. Moosavi-Dezfooli, J. Lai, and X. Xie, "The enemy of my enemy is my friend: Exploring inverse adversaries for improving adversarial training," in *Proceedings of the IEEE/CVF Conference on Computer Vision and Pattern Recognition*, 2023, pp. 24 678–24 687.

[36] Q. Li, Y. Guo, W. Zuo, and H. Chen, "Squeeze training for adversarial robustness," in *International Conference on Learning Representations*, 2023.

[37] Y. Mo, D. Wu, Y. Wang, Y. Guo, and Y. Wang, "When adversarial training meets vision transformers: Recipes from training to architecture," in *Neural Information Processing Systems*, 2022.

[38] Z. Wei, Y. Wang, Y. Guo, and Y. Wang, "CFA: class-wise calibrated fair adversarial training," in *CVPR*, 2023, pp. 8193–8201.

[39] T. Chen, Z. Zhang, S. Liu, S. Chang, and Z. Wang, "Robust overfitting may be mitigated by properly learned smoothening," in *ICLR*, 2021.

[40] P. Izmailov, D. Podoprikhin, T. Garipov, D. P. Vetrov, and A. G. Wilson, "Averaging weights leads to wider optima and better generalization," in *UAI*, A. Globerson and R. Silva, Eds., 2018, pp. 876–885.

[41] H. Wang and Y. Wang, "Generalist: Decoupling natural and robust generalization," in *Proceedings of the IEEE/CVF Conference on Computer Vision and Pattern Recognition*, 2023, pp. 20 554–20 563.

[42] A. Krizhevsky *et al.*, "Learning multiple layers of features from tiny images," 2009.

[43] Y. Netzer, T. Wang, A. Coates, A. Bissacco, B. Wu, and A. Y. Ng, "Reading digits in natural images with unsupervised feature learning," in *Neural Information Processing Systems Workshop on Deep Learning and Unsupervised Feature Learning*, 2011.

[44] S. Zagoruyko and N. Komodakis, "Wide residual networks," in *BMVC*, 2016.

[45] A. Dosovitskiy, L. Beyer, A. Kolesnikov, D. Weissenborn, X. Zhai, T. Unterthiner, M. Dehghani, M. Minderer, G. Heigold, S. Gelly *et al.*, "An image is worth 16x16 words: Transformers for image recognition at scale," in *International Conference on Learning Representations*, 2020.

[46] H. Touvron, M. Cord, M. Douze, F. Massa, A. Sablayrolles, and H. Jégou, "Training data-efficient image transformers & distillation through attention," in *International Conference on Machine Learning*, 2021, pp. 10 347–10 357.

[47] S. d'Ascoli, H. Touvron, M. L. Leavitt, A. S. Morcos, G. Biroli, and L. Sagun, "Convit: Improving vision transformers with soft con-

volutional inductive biases," in *International Conference on Machine Learning*, 2021, pp. 2286–2296.

Xin Liu received the B.S. degree in computer science and technology from Huazhong University of Science and Technology, Wuhan, China, in 2022. He is pursuing the M.S. degree with the School of Computer Science and Technology, Huazhong University of Science and Technology, Wuhan, China. His interests include deep learning and adversarial machine learning.

Yichen Yang received the B.S. degree in computer science and technology from Huazhong University of Science and Technology, Wuhan, China, in 2020. He is pursuing the M.S. degree with the School of Computer Science and Technology, Huazhong University of Science and Technology, Wuhan, China. His interests include deep learning and adversarial machine learning.

Kun He (SM18) is currently a Professor in School of Computer Science and Technology, Huazhong University of Science and Technology, Wuhan, P.R. China. She received her Ph.D. in system engineering from Huazhong University of Science and Technology, Wuhan, China, in 2006. She had been with the Department of Management Science and Engineering at Stanford University in 2011-2012 as a visiting researcher. She had been with the department of Computer Science at Cornell University in 2013-2015 as a visiting associate professor, in 2016 as a visiting professor, and in 2018 as a visiting professor. She was honored as a Mary Shepard B. Upson visiting professor for the 2016-2017 Academic year in Engineering, Cornell University, New York. Her research interests include adversarial machine learning, deep learning, graph data mining, and combinatorial optimization.

John E. Hopcroft (Fellow 1987, Life Fellow 2004) is the IBM Professor of Engineering and Applied Mathematics in Computer Science at Cornell University. After receiving both his M.S. (1962) and Ph.D. (1964) in electrical engineering from Stanford University, he spent three years on the faculty of Princeton University. He joined the Cornell faculty in 1967, was named professor in 1972 and the Joseph C. Ford Professor of Computer Science in 1985. He was honored with the A. M. Turing Award in 1986. He is a member of the National Academy of Sciences (NAS), the National Academy of Engineering (NAE), a foreign member of the Chinese Academy of Sciences, and a fellow of the American Academy of Arts and Sciences (AAAS), the American Association for the Advancement of Science, the Institute of Electrical and Electronics Engineers (IEEE), and the Association of Computing Machinery (ACM). Hopcroft's research centers on theoretical aspects of computing, especially analysis of algorithms, automata theory, and graph algorithms. His most recent work is on the study of information capture and access.